Available online at www.sciencedirect.com

ScienceDirect

Mendeleev Commun., 2020, **30**, 285–287

Mendeleev Communications

XPS study of interactions between linear carbon chains and colloidal Au nanoparticles

Ivan S. Zhidkov,*[a] Ernst Z. Kurmaev,[a,b] Seif O. Cholakh,[a] Enza Fazio[c] and Luisa D'Urso[d]

[a] *Institute of Physics and Technology, Ural Federal University, 620002 Ekaterinburg, Russian Federation. E-mail: i.s.zhidkov@urfu.ru*

[b] *M. N. Mikheev Institute of Metal Physics, Ural Branch of the Russian Academy of Sciences, 620990 Ekaterinburg, Russian Federation*

[c] *Dipartimento di Scienze Matematiche e Informatiche, Scienze Fisiche e Scienze Della Terra (MIFT), Università di Messina, 98166 Messina, Italy*

[d] *Dipartimento di Scienze Chimiche, Università di Catania, 95125 Catania, Italy*

DOI: 10.1016/j.mencom.2020.05.007

The X-ray photoelectron spectra (XPS) of Au colloidal nanoparticles (Au NPs) and Au–NPs/linear carbon chain (LCC) structures (Au@LCC) prepared by nanosecond pulsed laser ablation in liquid water were measured. The Au 4*f* XPS peaks of Au NPs coincided with those of metallic gold to confirm that a metallic state was retained in colloidal Au nanoparticles. On the other hand, the Au 4*f* XPS spectra of Au@LCC showed a low-energy broadening due to the formation of Au–C bonds between Au NPs and LCC.

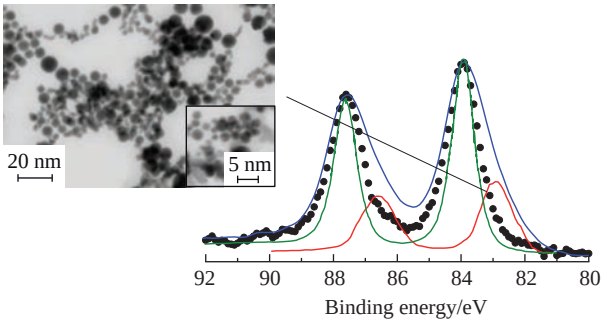

Keywords: XPS, linear carbon chains, Au nanoparticles, electronic structure, oxidation.

Metal nanoparticles (NPs) are of great interest due to their physical and chemical properties different from those of the bulk counterparts.[1–3] Gold nanoparticles (Au NPs) are remarkable[4,5] because of potential applications in catalysis,[6,7] biomedicine,[8–10] and optics.[11,12] Colloidal Au NPs can be used in medicine, sensing, imaging, and therapy due to their biocompatibility and optical properties associated with localized surface plasmon resonances.[13–17] Various stabilizers, such as donor ligands, polymers, and surfactants, are used to control the growth of Au NPs and to prevent them from agglomeration. The surface modification of Au NPs and their stabilizing functional groups are of interest due to the possibility of controlling their colloidal and chemical behaviors. We studied the interaction of sp^1 linear carbon chains (LCCs) with colloidal Au NPs† using X-ray photoelectron spectroscopy (XPS),‡ which gives direct information on local atomic and electronic properties of excited atoms.

Scanning transmission electron microscopy (STEM)§ was used for studying the sizes and agglomeration of NPs. Figure 1 shows STEM micrographs and size distribution histograms of Au NPs and Au@LCC hybrid nanostructures. The Au NPs exhibited a shape anisotropy due to aggregation phenomena with elongated structures from 10 to 80 nm in length. Polydispersed NPs were composed of spherical NP aggregates about 20 nm in diameter [Figure 1(*b*)]. The Au@LCCs were spherical with a narrow size distribution centered at about 8 nm. Note that average diameters slightly decreased from 20 to 8 nm when LCCs were prepared in the presence of Au NPs. This tendency can be simply explained in terms of size reduction induced by a second laser irradiation process. These observations indicate that Au NPs of controlled shape and size were prepared, hindering the formation of elongated aggregates by LCCs protection.

Figure 2 shows the survey XPS spectra, which exhibited C, O, Si, and Au signals, and only trace nitrogen and copper impurities were detected. The concentration of polyynes $(–C{\equiv}C–)_n$ in the solution was estimated from these spectra (Table 1). The polyyne amount in water solution was calculated from UV-VIS spectral data using published molar extinction coefficients.[20] Generally consistent amounts of amorphous carbon were also observed in the presence of LCCs after deposition and exposure to air (solid

† Surfactant-free Au NPs and Au/linear carbon chain LCC (core/shell) structures were prepared using nanosecond pulsed laser Nd:YAG 532 nm (operating at a repetition rate of 10 Hz with a pulse width of 5 ns) ablation (PLA) in liquid water. For the preparation of Au@LCCs, the same metal colloidal dispersion was used to ablate a polycrystalline graphite (99.99% purity) target.[18] The LCCs were characterized by alternating single and triple bonds (general formula C_nH_2):LLC with n = 6, 8 and identified from UV-VIS spectra ESI.[18,19] Almost all gold nanoparticles are encapsulated to a shell as confirmed by the transmission electron microscopy analysis based on the absence of coagulation.[18]

‡ XPS core-level and valence band (VB) measurements were performed using a PHI 5000 VersaProbe XPS spectrometer (ULVAC Physical Electronics, USA) based on a classic X-ray optic scheme with a hemispherical quartz monochromator and an energy analyzer working in a binding energy range of 0 to 1500 eV. This apparatus uses electrostatic focusing and magnetic screening to achieve an energy resolution of $\Delta E \leqslant 0.5$ eV for AlKα radiation (1486.6 eV). The analytical chamber was pumped down using an ion pump to a pressure lower than 10^{-7} Pa. The XPS spectra were recorded using AlKα X-ray emission. The spot size was 200 μm, and the X-ray power load delivered to the sample was < 50 W. Typical signal-to-noise ratios were greater than 10000:3.

§ The STEM analysis was carried out with a Zeiss-Gemini 2 electron microscope operating at 150 kV.

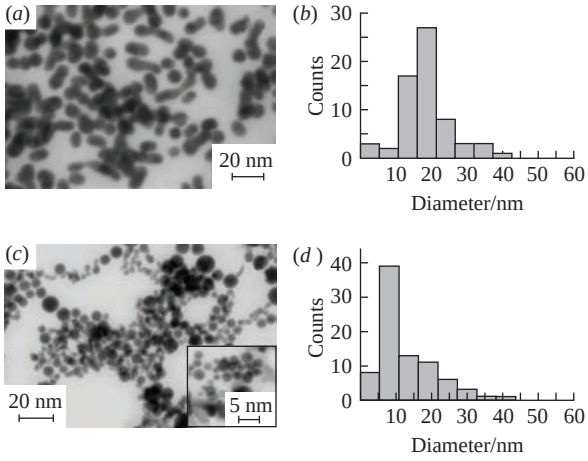

Figure 1 STEM micrographs of (*a*) as-prepared Au and (*c*) Au@LCC nanostructures and (*b*, *d*) the size distribution histograms.

state analysis); in liquid, the main species adsorbed were LCCs, as confirmed by SERS measurements.[18] The concentration of Au colloids in water was estimated at about 0.3×10^{-6} M.

Figure 3 depicts the high-resolution Au 4*f* XPS spectra of Au NPs and Au@LCCs. Two peaks at 83.9 and 87.5 eV in the spectra of Au NPs correspond to Au $4f_{7/2}$ and $4f_{5/2}$ signals, respectively, in the gold metal.[21] This confirms that Au NPs retain in the metallic state in colloid solutions. At the same time, the Au 4*f* XPS spectra of Au@LCCs show noticeable broadening in a lower energy region, while maintaining the energy position of the main lines coinciding with the position of metallic gold reference. This behavior could be caused by an additional 4*f* doublet at binding energies of ~82.9 and ~86.5 eV.

Similar low-energy shifts of Au 4*f* XPS peaks were observed previously in gold nanoparticles deposited on single-walled carbon nanotubes (Au@SWCNT) (see Figure 3) and attributed to Au–C bonding.[22] Note that the low-energy contributions in the Au 4*f* XPS spectra of Au@LCCs cannot be due to the oxidation of Au nanoparticles because the Au 4*f* spectra of Au_2O_3 are shifted to an opposite side by 85.9 and 89.5 eV.[23] Therefore, in compliance with published data,[22] we concluded that the appearance of additional low-energy contributions of the Au 4*f* spectra in Au@LCC was due to the formation of Au–C bonds because of strong electrostatic

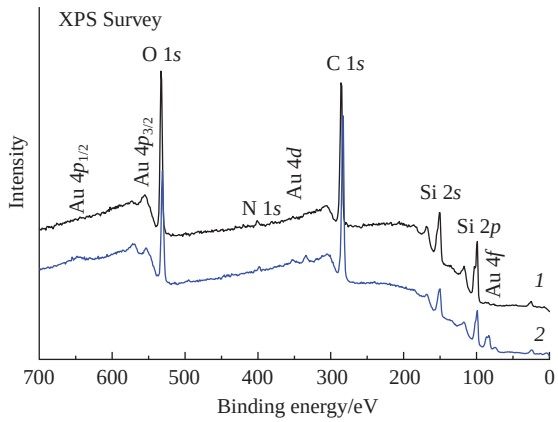

Figure 2 XPS survey spectra of (*1*) Au and (*2*)Au@LCC nanoparticles.

Table 1 Surface composition of Au and Au@LCC nanoparticles.

Sample	C (at%)	O (at%)	Si (at%)	Cu (at%)	Au (at%)	N (at%)
Au NP	54.1	24.6	19.9	0.3	0.1	1.0
Au@LCC	66.6	19.1	12.0	1.2	0.3	0.7

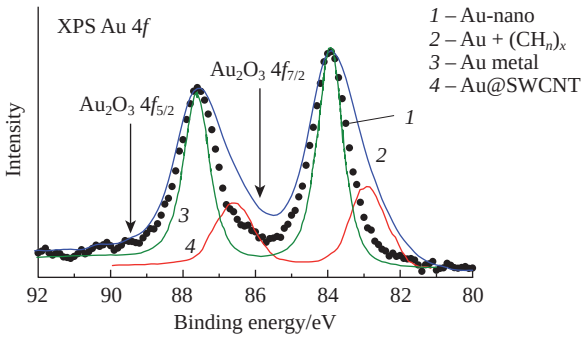

Figure 3 Au 4*f* XPS spectra of Au NPs and Au@LCC *vs.* that of Au@SWCNT from ref. 22.

and dispersive interactions between Au NPs and LCCs. This is consistent with XPS measurements of water-dispersible silver nanoparticles stabilized by metal–carbon bonds where the formation of Ag–C bonding was observed.[24,25]

For clarifying possible formation of Au–O bonds, the O 1*s* XPS spectra were measured [Figure 4(*b*)] and they were found very similar for Au and Au@LCC nanoparticles. The adsorption of water on the surfaces of Au NPs and Au@LCC can be responsible for the main peak (531.8 eV), which is in good agreement with O 1*s* of [OH]-related species.[26] We did not observe the signals of gold oxide in the O 1*s* spectra and/or C–O (C=O) bonds in the C 1*s* spectra (Figure 4). Thus, we can conclude that there is no XPS evidence for the oxidation of Au NPs or Au@LCC and the formation of C–O and C=O bonds. Attention should be paid to a weak signal at E_b = 282.9 eV, which corresponds to the C 1*s* peak position of LCC.[27]

Furthermore, XPS VB spectra also could evidence the formation of Au–C bonds in Au@LCC NPs. We compared the XPS VB of Au@LCC NPs (Figure 5) and those of metallic Au[28] and found that they are noticeably different in the intensity of a low-energy peak (~3 eV). This peak intensity most probably increased due to the formation of Au–C bonds. Note that the appearance of an additional C 2*s* subband was detected. The energy difference of these features (9.12 eV) is close to the difference between C 2*p* and C 2*s* orbital energies (ΔE = 8.5 eV) in free carbon atoms.[29] This fact is also consistent with our assumption on the formation of Au–C bonds in Au@LCC nanoparticles.

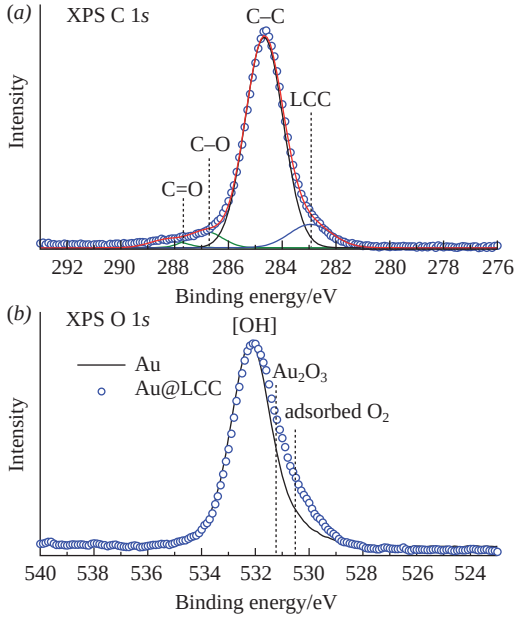

Figure 4 (*a*) C 1*s* and (*b*) O 1*s* XPS spectra of Au and Au@LCC nanoparticles.

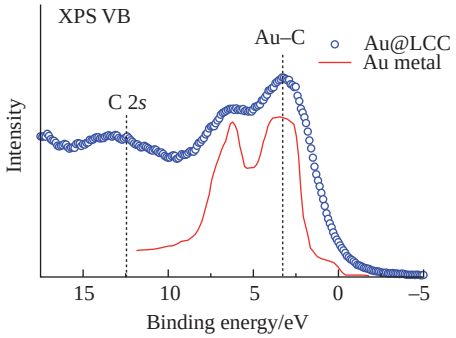

Figure 5 XPS VB spectra of Au and Au@LCC nanoparticles.

Thus, our XPS measurements showed that the Au 4*f* spectra of Au@LCCs were significantly modified in comparison with those of unreacted Au NPs due to the strong interaction of linear carbon chains with Au NPs and the formation of Au–C bonds. We demonstrated the possibility of protecting chemically unstable low-dimensional systems by forming composites with linear carbon chains, which increase the stability of Au NPs and prevent their agglomeration.

This study was supported by the Russian Science Foundation (project no. 19-72-00001).

References

1 *Nanoparticles. Building Block for Nanotechnology*, ed. V. Rotello, Kluwer Academic Publishers, New York, 2004.
2 *Nanoparticles: From Theory to Application*, ed. G. Schmid, Wiley-VCH, Weinheim, 2006.
3 C. Burda, X. Chen, R. Narayanan and M. A. El-Sayed, *Chem. Rev.*, 2005, **105**, 1025.
4 *Gold Nanoparticles for Physics, Chemistry and Biology*, eds. C. Louis and O. Pluchery, Imperial College Press, London, 2012.
5 P. Zhao, N. Li and D. Astruc, *Coord. Chem. Rev.*, 2013, **257**, 638.
6 M. Haruta and M. Daté, *Appl. Catal., A*, 2001, **222**, 427.
7 A. Corma and P. Serna, *Science*, 2006, **313**, 332.
8 Y.-C. Yeh, B. Creran and V. M. Rotello, *Nanoscale*, 2012, **4**, 1871.
9 E. C. Dreaden, A. M. Alkilany, X. Huang, C. J. Murphy and M. A. El-Sayed, *Chem. Soc. Rev.*, 2012, **41**, 2740.
10 E. N. Shapovalova, A. D. Golubova, I. A. Ananieva, T. M. Baygildiev and O. A. Shpigun, *Mendeleev Commun.*, 2019, **29**, 702.
11 F. Hajizadeh and S. N. S. Reihani, *Opt. Express*, 2010, **18**, 551.
12 H. Dai, L. Zhang, Z. Wang, X. Wang, J. Zhang, H. Gong, J.-B. Han and Y. Han, *J. Phys. Chem. C*, 2017, **121**, 12358.
13 S. A. Abdulateef, A. F. Omar, M. Z. Mat Jafri, N. M. Ahmed and A. Seeni, *J. Cluster Sci.*, 2017, **28**, 3193.
14 M. Vinod, R. S. Jayasree and K. G. Gopchandran, *Curr. Appl. Phys.*, 2017, **17**, 1430.
15 V. Garg, B. S. Sengar, V. Awasthi, Aaryashree, P. Sharma, C. Mukherjee, S. Kumar and S. Mukherjee, *RSC Adv.*, 2016, **6**, 26216.
16 V. Amendola, R. Pilot, M. Frasconi, O. M. Maragò and M. A. Iatì, *J. Phys.: Condens. Matter*, 2017, **29**, 203002.
17 L. A. Dykman and N. G. Khlebtsov, *Russ. Chem. Rev.*, 2019, **88**, 229.
18 L. D'Urso, G. Grasso, E. Messina, C. Bongiorno, V. Scuderi, S. Scalese, O. Puglisi, G. Spoto and G. Compagnini, *J. Phys. Chem. C*, 2010, **114**, 907.
19 E. Fazio, F. Neri, S. Patanè, L. D'Urso and G. Compagnini, *Carbon*, 2011, **49**, 306.
20 T. R. Johnson and D. R. M. Walton, *Tetrahedron*, 1972, **28**, 5221.
21 J. F. Moulder, W. F. Stickle, P. E. Sobol and K. D. Bomben, *Handbook of X-ray Photoelectron Spectroscopy*, ed. J. Chastain, Perkin-Elmer Corp., Eden Prairie, MN, 1992.
22 M. K. Bayazit, S. A. Hodge, A. J. Clancy, R. Menzel, S. Chen and M. S. P. Shaffer, *Chem. Commun.*, 2016, **52**, 1934.
23 K. Juodkazis, J. Juodkazyte, V. Jasulaitiene, A. Lukinskas and B. Sebeka, *Electrochem. Commun.*, 2000, **2**, 503.
24 K. Kawai, T. Narushima, K. Kaneko, H. Kawakami, M. Matsumoto, A. Hyono, H. Nishihara and T. Yonezawa, *Appl. Surf. Sci.*, 2012, **262**, 76.
25 D. W. Boukhvalov, I. S. Zhidkov, E. Z. Kurmaev, E. Fazio, S. O. Cholakh and L. D'Urso, *Carbon*, 2018, **128**, 296.
26 A. Kossoy, H. Cohen, T. Bendikov, E. Wachtel and I. Lubomirsky, *Solid State Ionics*, 2011, **194**, 1.
27 T. Danno, Y. Okada and J. Kawaguchi, *AIP Conf. Proc.*, 2004, **723**, 431.
28 H. Piao and N. S. Mcintyre, *J. Electron. Spectrosc. Relat. Phenom.*, 2001, **119**, 29.
29 F. Herman and S. Skillman, *Atomic Structure Calculations*, Prentice-Hall, Englewood Cliffs, NJ, 1963.

Received: 25th November 2019; Com. 19/6066